# 3D Dynamic Opto-mechanical Modeling of Diode-pumped Trapezoid Yb:YAG/YAG Thin Disk Laser

H. Aminpour[1,2,*] and C. Pflaum[1,2]
[1]Graduate School in Advanced Optical Technologies (SAOT), Friedrich-Alexander University of Erlangen-Nuremberg, Paul-Gordan-Str.6, 91052 Erlangen, Germany
[2]Department of Computer Science Informatics 10, System Simulation (LSS),
University of Erlangen-Nuremberg, Cauerstr.11 91058 Erlangen, Germany
*Hamed.amin.pour@fau.de

*Abstract*— **We present a 3D modeling of thermal lensing effect in an edge-pumped trapezoid Yb:YAG/YAG thin disk laser. At first, a Monte-Carlo ray tracing method is used to calculate the absorbed pump power from four sides in such a way that the pump light are totally trapped inside the crystal after total reflections. Secondly, we optimized the absorption efficiency of our laser which is obtained 66.7% with Yb:YAG dopant of 10% and efficient thickness of 0.2mm. Then, using the result of absorbed pump light distribution to compute temperature distribution inside the crystal and fulfill the consequence of opto-mechanical properties including Von Mises stress and deformation components distribution inside the crystal via Finite Element Analysis (FEA). Furthermore, the thermal lens power is considered in our modeling as an important consequence of opto-mechanical effect and compared in different output powers. Finally, we applied the Dynamic Multimode Analysis (DMA) method to solve the rate equation and calculate the output powers respect to different length of cavities and different output coupler curvatures respect to the dealing beam quality in multimode operation.**

**Keywords- Ytterbium laser; Thermal effects; Solid-state laser; Diode-pumped laser**

## I. INTRODUCTION

Power scalability and minimal thermal lensing are the particular features of thin disk lasers. High output power, high efficiency and good beam quality are further advantageous of this type of solid - state laser [1,3]. So far, thin disk lasers with multi-kilowatt output powers and multi-mode operation are discussed too many in articles and advanced to a common tool for cutting, welding and material processing in industries. Nowadays, interests has been shifted towards a significant enhancement of the beam quality of this type of laser [4]. Unlike in side pumped rod laser materials, thermal gradient and laser output beam are in the same direction in conventional thin disk lasers [5, 6] so, the thermal lens effect is not negligible in thin disk lasers.

Also, the absorbed pump power density increase the temperature in the gain medium and correspondingly inhomogeneous pumping creates a non-uniform temperature distribution inside the crystal. On the other hand, owing to the randomness of ray propagation and exponential absorption of the pump light, the temperature inhomogeneity arise in different parts of the disk. These temperature differences cause a thermal lens effect which distorts the wave front of the laser beam. So, in modeling, thin disk laser resonator can be considered as a resonator containing internal lenses with additional thermo-optical effects such as optical path difference and phase distortion which can considerably affect the laser beam quality. It has been shown that the effects of thermal lens on laser wave front in thin disk laser at high power operation mode can be compensated by applying an appropriate output coupler curvature in the resonator [7]. Since thermal effects including stress fracture and thermal lensing are the main limiting factors to laser output power and beam quality of solid state lasers [8]. They are some of the most critical issues to be considered in the resonator design to reduce and compensate the influence of these aberrations. Nevertheless, the main advantage of thin disk laser is the efficient cooling of the laser medium due to the big ratio of surface to volume [9].The end pump disk laser requires complex pumping equipment to achieve multi-pass pumping, whereas in edge pumped thin disk laser efficient absorption length is achieved more easily and there is not any need to use complicated pumping setups [10]. Pumping can be done by simply focusing the diode light into the active medium by use of lenses or use an alternative lens duct [11, 12].The edged pumped thin disk lasers assure efficient absorption length, simple pump configuration and pump beam shaping which is explicit [13]. Recently different crystal structures such as microchip composite and ceramic microchips have been reported for efficient edged pumped thin disk laser [14]. Following according these approaches, in this current work, we present a novel edged pumped trapezoid shape of thin disk laser and modeling the opto-mechanical behavior of our delivery system in more details.

## II. MODEL CHARACTERIZATION

In this work, we used an edge diode pumped Yb:YAG/YAG trapezoid thin disk laser with slant angle of 30 degree. The dimensions of the gain medium is 8×8×0.2 mm. Each sides of the disk are inclined at 30 degree with respect to the optical axis so that the pump beam propagate along the disk in zigzag path allowing multi-pass of the pump beam inside the gain medium Fig.1.

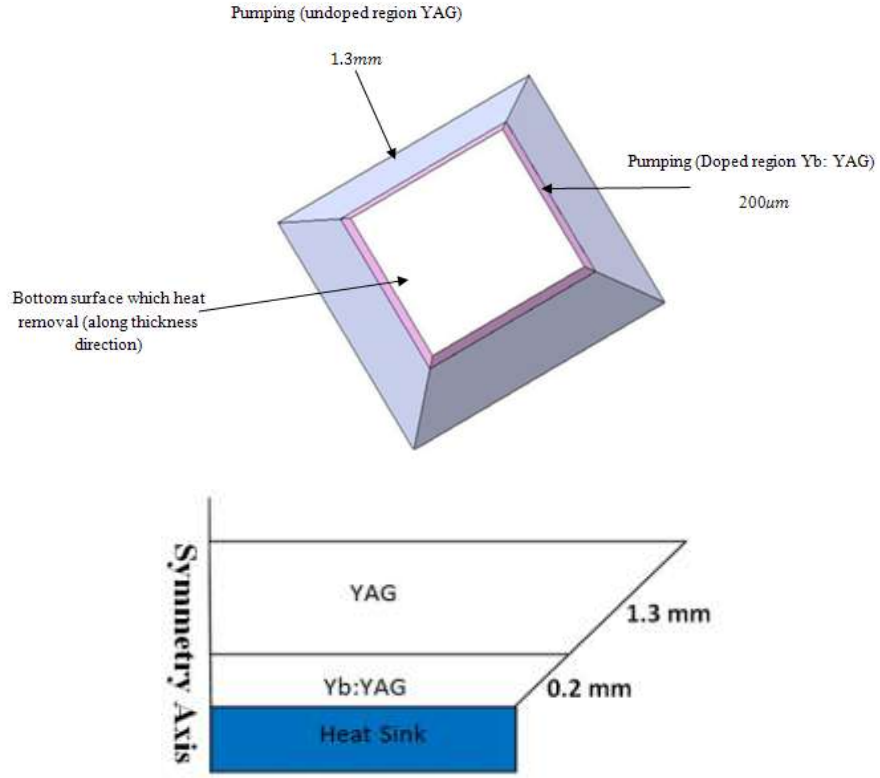


Figure 1. Isometric layout of the gain medium and half side cross-section view of the gain medium.

Our crystal is pumped by four diode arrays after propagation through the hollow ducts which are placed outside the trapezoid Yb:YAG/YAG crystal. The output power of each pump diode bars was taken in range of 12.5-125W resulting a total pump power range of 50-500W with the fast axis divergence about 10 degree and slow axis divergence about 0.25 degree inside the crystal Fig.2 illustrates in more detail the propagation of the pump light inside the active medium for more clarity. In addition, an undoped cap of YAG crystal with 1.3mm thickness is bonded on the top of the active medium in one hand to improve the mechanical stiffness, displacement and stress components of the crystal, on the other hand to help for better conducting of thermal from top surface of the gain medium. Due to our specific geometry a total internal refection (TIR) routinely tack place with the pumping arrangement that is used in our modeling [15]. Another advantage of our geometry is that, there is no need to use any coated surface to reflect pump wavelength on the internal face of the upper surface of the disk Fig 2.

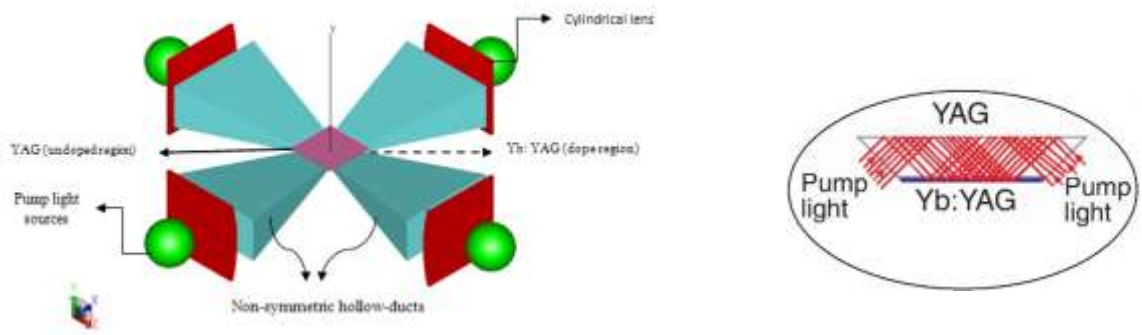


Figure 2. Isometric Schematic view of sources and four hollow ducts used for pumping the active medium from four slanted sides.

Finally, the crystal inserted in a linear cavity of 460mm with the output coupler curvature of 1m and the reflection of 88%. The bottom surface of the Yb:YAG/YAG crystal is high-reflection (HR) coated at 1030nm and 940nm. The heat load deposited in the active medium is removed by cooling water of 286K from the bottom surface Fig.3. More parameters of our thin disk laser are listed in Table I.

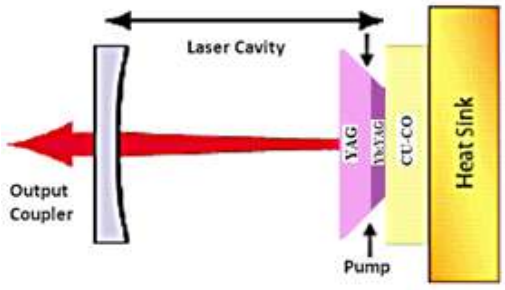


Figure 3. Schematic view of our disk configuration placed inside the linear cavity and cooling from the bottom surface.

TABLE I. PARAMETERS OF TRAPEZOID DISK CRYSTAL USED IN OUR MODELING

| **Parameter** | **Value** | **Unit** |
|---|---|---|
| Side length | 8 | mm |
| Thickness of doped region | 0.2 | mm |
| Thickness of un-doped region | 1.3 | mm |
| $Yb^{+3}$ concentration | 10 | % |
| Thermal exchange coef. disk/heat sink | $8\times10^{4}$ | $W/m^2K$ |
| Thermal exchange coef. disk/air [16] | 10 | $W/m^2K$ |
| Thermal resistances [3] | 12.7 | $Kmm^2/W$ |
| Coolant temperature($T_c$) | 286 | K |
| Ambient temperature ($T_a$) | 300 | K |
| Refractive index (Yb:YAG) | 1.82 | ------- |
| Total pump power | 50-500 | W |
| Heat fraction[16] | 14.6 | % |
| Yang modulus (E) of Yb:YAG [16] | 310 | GPa |
| Poison ratio (x,y,z components) [17] | 0.3 | ------- |
| Tensile Strength (Yb:YAG) | 130-260 | MPa |
| dn/dT [17] | $7.3\times10^{-6}$ | 1/K |

### *A. Modeling algorithm*

We have used the following algorithm in our modeling Fig.4. First, we used Monte-Carlo ray tracing method to simulate the pump light source distribution inside the volume of the crystal with the central wavelength of 940nm. The first step has been done in our developing simulation code ASLD software [18]. Then, we calculated the absorption pump light density inside the active medium using Reciprocity method. After that the result of the previous step is used to determine the heat source inside the crystal to calculate the temperature and the opto-mechanical properties of our gain medium such as stress, deformation and OPD by using Finite Element Analysis (FEA) method. Finally, we used Dynamic Multi-mode Analysis (DMA) to calculate the output power and beam quality of our laser.

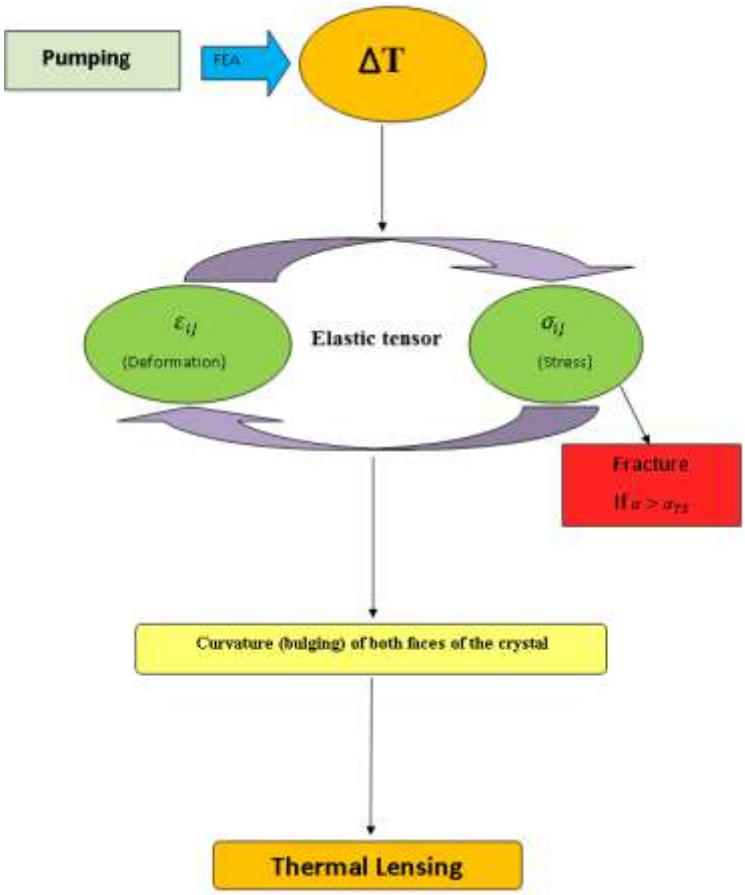


Figure 4. The algorithm procedure used in our modeling.

## III. ABSORBED PUMP LIGHT DISTRIBUTION

In this section, we have done the Monte-Carlo ray tracing with the aim of creating an uniform and homogeneous distribution of pump light inside the crystal. We simulated the pump light distribution in Trace Pro ray tracing software [19] which result is depicted in Fig.5. In the following, we obtained the absorption efficiency of our laser due to different Yb:YAG dopant. As a result of our simulation, we obtained an efficient Yb:YAG dopant of 10% which is shown in Fig.6. As shown in Fig.6 the absorbed pump power is enhanced exponentially and become constant for the dopant of 10%. So, we have chosen the dopant of 10% as an optimum case for our active medium and did the following simulation respect to this calculation. Also the average absorption efficiency of 66.7% for our laser system has been obtained simultaneously. Furthermore, we continued our simulation for the pump power range of 100-1000W which is shown in Fig.7.

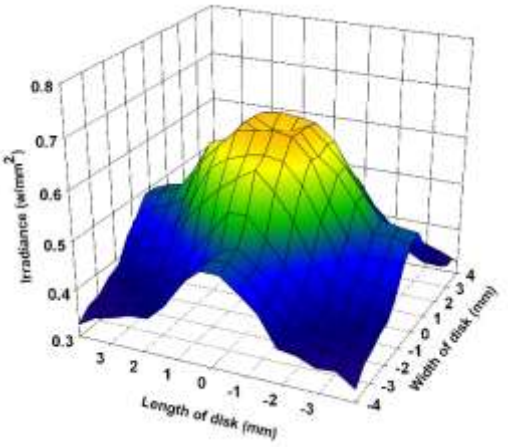


Figure 5. Pump light distribution profile inside the crystal obtained by ray tracing in TracePro.

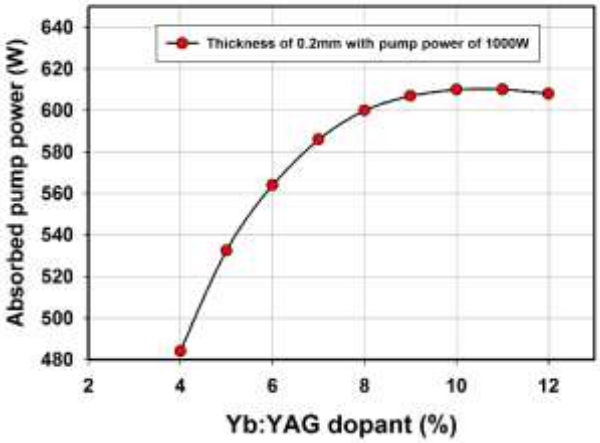


Figure 6. Pump Absorption pump power versus different Yb:YAG dopants.

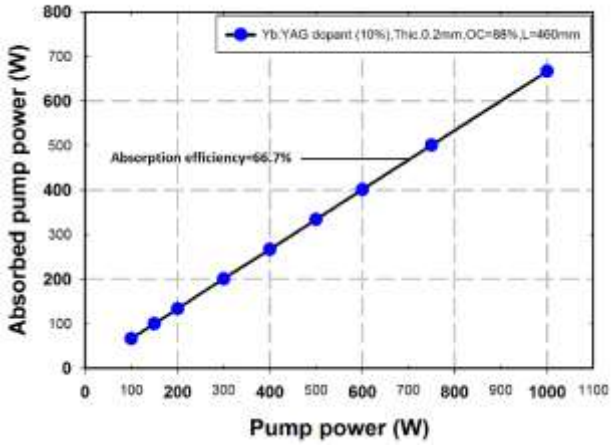


Figure 7. Absorbed pump power efficiency versus output powers

## IV. TEMPERATURE DISTRIBUTION

Thermal effects calculation inside the crystal are considered by finite element analysis (FEA). In this section of our modeling, we follow the following critical steps:

- Determination of heat load distribution
- Solution of 3D differential equations of heat conduction
- Solution of the differential equation of structural deformation

For this calculation, the amount of absorbed pump power from previous section is assumed to be converted into heat power density inside the active medium which representing the source of the thermal lensing in the following steps of our modeling. The differential equations of heat conduction determine as: [20]

$$-\nabla.[(K(T)\nabla(T)] = Q(x,y,z) \tag{1}$$

$$\frac{dT}{dZ} = [T_c - T_s]\frac{h_c}{K(T)} \qquad \text{at } z = 0$$

$$\frac{dT}{dx} = [T_a - T_s]\frac{h_a}{K(T)}$$

$$\frac{dT}{dy} = [T_a - T_s]\frac{h_a}{K(T)} \tag{2}$$

In Eq.1 and 2, index ,S, stands for the slanted faces of the disk (except for the bottom face). Where ,$h_a$, (10 $W/m^2K$) is the free convection heat transfer coefficient on edges and on the top surface of the active medium (between air and the disk), $h_c$ ($8 \times 10^4$ $W/m^2K$ ) is a convection heat transfer coefficient on the bottom face which is connected to the heat sink ,$T_c$ , is the coolant temperature (286K), $T_a$ , is the ambient room temperature (300K), $T_S$ is the temperature of the slanted faces and the top surface of the crystal. Q(x,y,z) is the heat energy deposited per unit volume which in our modeling it is taken as proportional to the absorbed pump power density distribution inside the active medium. Our modeling shows that the temperature decreases when going outwards from the center of the disk to the side faces due to the fact that pump light is focused entirely in the center of the disk which is shown in Fig.8. Furthermore, the temperature gradient along the thickness for the doped region (Z=0 to Z=0.2 mm) increases because of the bottom surface of the disk is cooled by the heat sink.

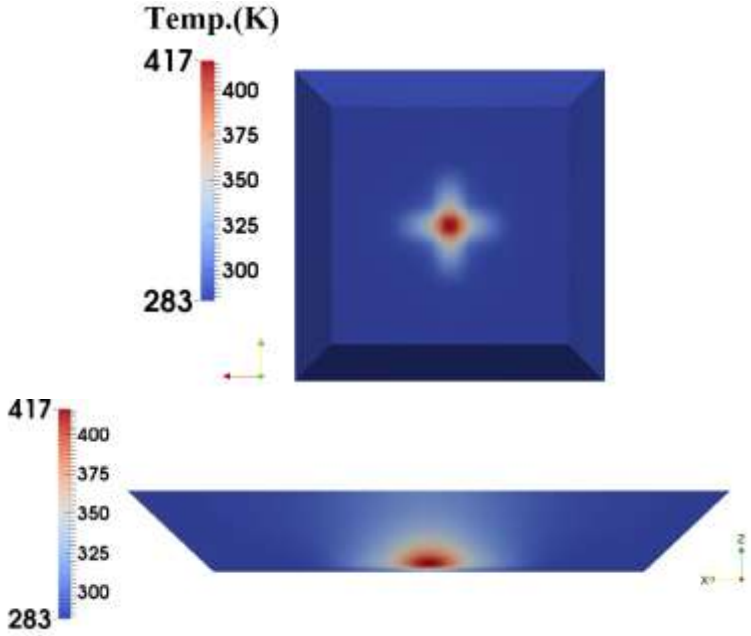


Figure 8. Temperature distribution profile inside the crystal from the bottom cross section view and from the side cross section view

## V. VON MISES STRESS DISTRIBUTION

Once the temperature distribution has been computed, the next step is to calculate the stress and strain distribution inside the crystal, obtained from the so-called generalized Hook law, which includes the thermal expansion term:[6]

$$\varepsilon_{ij} = S_{ijkl}\sigma_{kl} + \alpha T_{ij}\Delta T \tag{3}$$

Where, ΔT, is the temperature shift with respect to equilibrium (no strain), $S_{ijkl}$, is the compliance tensor,$\sigma_{kl}$, is the stress tensor ,$\varepsilon_{ij}$, is the strain tensor, and $\alpha T_{ij}$ is the tensor of thermal expansion coefficients. All principal components of the stress tensor are responsible for thermal gradient stress induced thermal lensing were then calculated by Finite Element Analysis (FEA). Our calculation shows the variation of ($\sigma_{zz}$) in the direction of laser beam increase at center of the crystal and decrease till it reaches through the slanted faces of the disk. Also, the ($\sigma_{xx}$) and ($\sigma_{yy}$) components of stress tensor are small in the center of the crystal. Furthermore, the modeling shows that the Von Mises stress is pretty small in our crystal which is shown in Fig.9 and is far below the fracture limit of such Yb:YAG crystal Table I. This behavior related to one of the benefits of our construction which used the un-doped cap upon the active medium. In our modeling, we used three different pump powers to compare the Von Mises stress which is depicted in Fig.10. From the distribution of Von Mises stress, one could see that the Von Mises stress variation is pretty smooth for 250W which is distributed approximately constant along the crystal. Whereas it varies drastically at the center of the disk by applying the pump light power of 500W and 1000W.

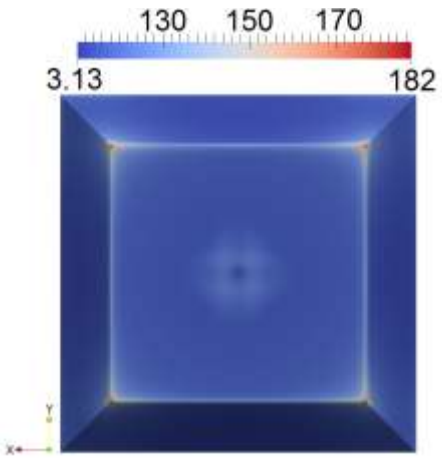


Figure 9. 3-dimensional Von Mises stress distributions on the bottom surface of the crystal.

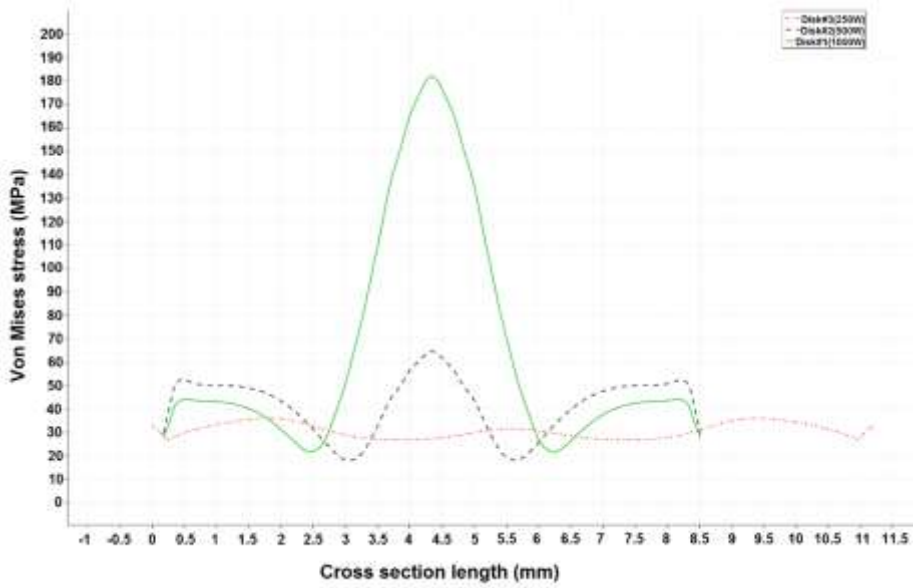


Figure 10. 2-dimensional comparison of Von Mises stress of disk in different pump powers on the top surface of the Yb:YAG crystal.

## VI. DEFORMATION DISTRIBUTION

Another effect that has an important role in changing the laser beam phase profile is deformation of the crystal. The displacement vector, $U_i$, is giving rise to the strain vector, $\varepsilon_{ik}$,. If ,$U_i$ , is small and for small deformations, the strain and displacement are given by the following equation:[21]

$$\varepsilon_{ik} = \frac{1}{2}\left(\frac{\partial U_i}{\partial x_k} + \frac{\partial U_k}{\partial x_i}\right) \tag{4}$$

We modeled the 3D deformation components (x,y,z) inside the crystal in different range of pump powers which results are illustrated in Fig.11 and Fig.12. These figures show the deformation distribution components on the top and the bottom surface of the crystal either in the direction of laser beam (z-direction), or in Y (length of the crystal) direction. Furthermore, we have done a 2D comparison which are depicted in Fig.13 and Fig.14. As shown in Fig.13, the maximum value of the Z-component of deformation for different pump powers varies which the highest value obtained 30.73µm for 1KW of pump power. Whereas this value in Z-direction is small comparing to the value in Y-direction (perpendicular to the laser beam direction) which is 60.7o µm. In addition, from Fig.13, one can see that the displacement in the center of the disk in Z-direction by increasing the pump power from 50W to1KW are drastically arise compare to the edges of the disk.

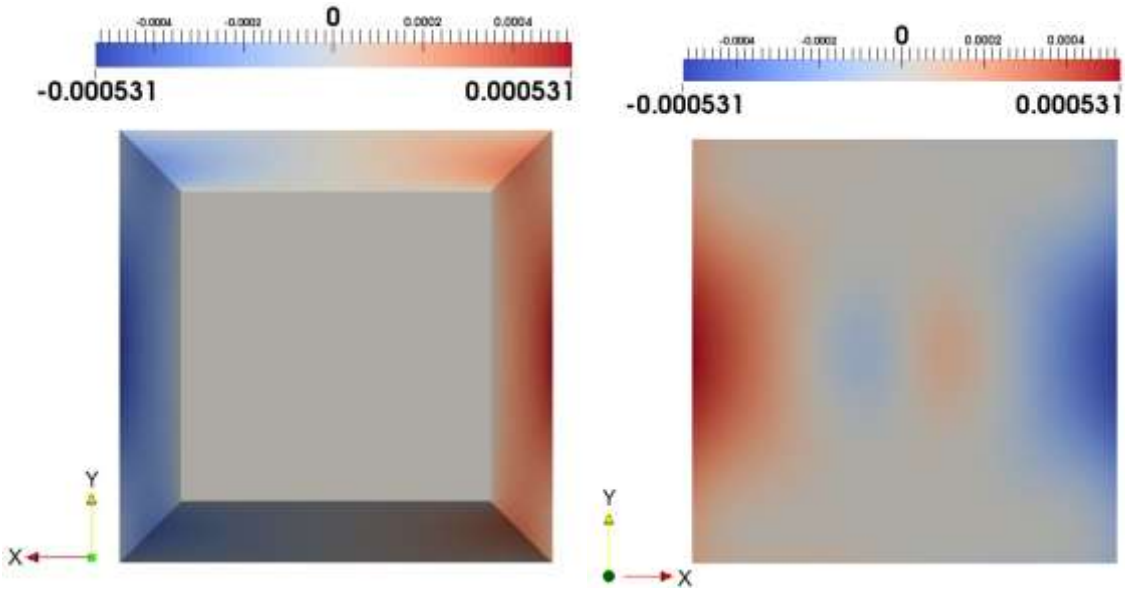


Figure 11. 3-dimensional deformation component distribution inside the crystal in X-direction (perpendicular to the laser beam direction) from the cross section view on top and bottom surface of the crystal.

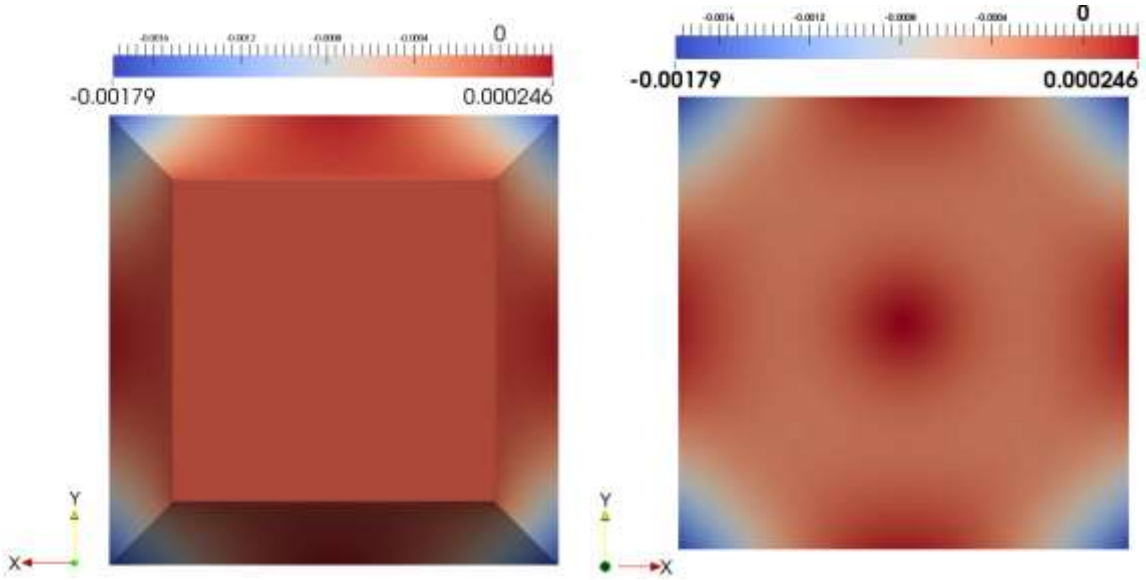


Figure 12. 3D deformation component distribution inside the crystal in Z-direction (parallel to the laser beam direction)

from the cross section view on top and bottom surface of the crystal.

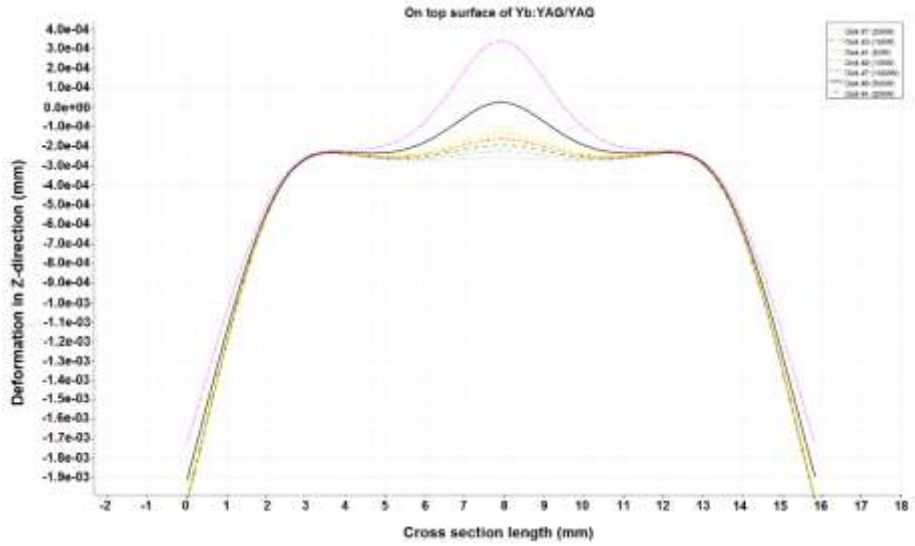


Figure 13. 2-dimensional comparison of Z-component deformation inside the crystal for different pump powers.

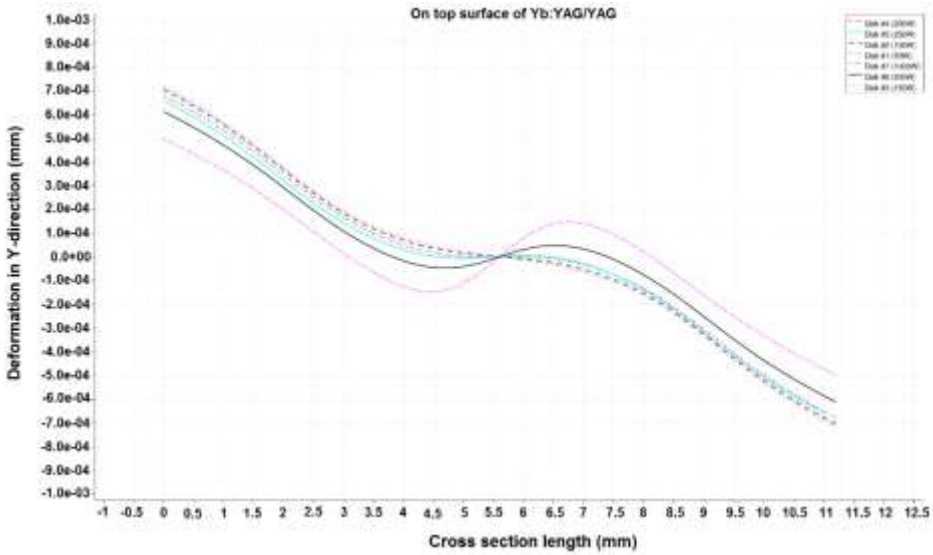


Figure 14. 2-dimensional comparison of Y-component of deformation inside the crystal for different pump powers.

## VII. OPTICAL PATH DIFFERENCE

Thermal lensing contains all the phenomena resulting in a phase change of a beam passing through a pumped crystal. Heating of the laser crystal often causes a significant thermal lens through the following mechanisms: [22, 24].

- The gain medium is hotter on the beam axis, compared with the outer regions, typically causing some transverse gradient of the refractive index (thermo-optic effect, quantified with the coefficient dn/dT)
- Further index changes can be caused by thermally induced mechanical stress.
- Solution of the differential equation of structural deformation Mechanical stress can also lead to bulging of the end faces of the gain medium (deformation), so that these also cause lensing which can be important for short laser crystals such thin disk lasers.

In this section, our goal is to obtain the consequence optical path difference (OPD) of our laser system. To do it in details, we consider a resonator containing internal lens in order to calculate the OPD which may cause important effect on laser beam quality. We have used the approach of the thick lens inside the cavity in our simulation that act as our active medium. Furthermore, this thick lens introduced by the change of the refractive index which is caused by temperature and a deformation dependent variation. The main contributors to the optical path difference (OPD) or thermal lensing in thin disk lasers are temperature gradients, thermal stress and

deformation. The change of the refractive index is a superposition of temperature and a stress- dependent variation. Hence we have:[25]

$$n(x,y,z) = n_0 + n(x,y,z)_T + n(x,y,z)_\varepsilon \tag{5}$$

Where, n(x,y,z), is the variation of refractive index, $n_0$, is the refractive index in the center of the disk , $n(x,y,z)_T$ and $n(x,y,z)_\varepsilon$ are temperature and stress-dependent refractive indices respectively. For a coherent beam profile which propagates in z-direction, the temperature-dependent variation due to the thermal dispersion, dn/dT , and the stress-dependent variation of refractive index which can be expressed as:

$$n(x,y,z)_T = T(x,y,z)\left(\frac{dn}{dT}\right) \tag{6}$$
$$n(x,y,z)_\varepsilon = \sum_{i,j=1}^{3} \frac{\partial n}{\partial \varepsilon_{ij}} \varepsilon_{ij}(x,y,z)$$

The physical distortion of the flatness surface of the disk, due to the deformation with the relative axial elongation $\partial U/_{\partial z}$ along z-direction is calculated as the value of $(n-1)\frac{\partial U(x,y,z)}{\partial z}$ [26].

Finally, distributions of temperature, strain, deformation cause a variation in the phase front for the light propagation through the crystal. The change in phase profile due to thermal effects leads to an increase or decrease in the curvature of the phase front after passing of the wave through the crystal. For most crystalline laser material including Yb:YAG the stress contributions to the refractive index are small. Therefore, in our modeling we consider only the temperature effect on the index of refraction. Using the results of the finite element analysis the OPD is calculated considering the deformation of the HR-bottom of the disk, the change of thickness due to thermal expansion and the change of the refractive index due to temperature and stress distribution. The value of the focal length of thermal lens inside the crystal due to the change of the refractive index respect to the different output powers is depicted in Fig.15. One could realize that its value inside the crystal increased from -3613.74mm to -542.85mm in the output power range of 30W to 250W.

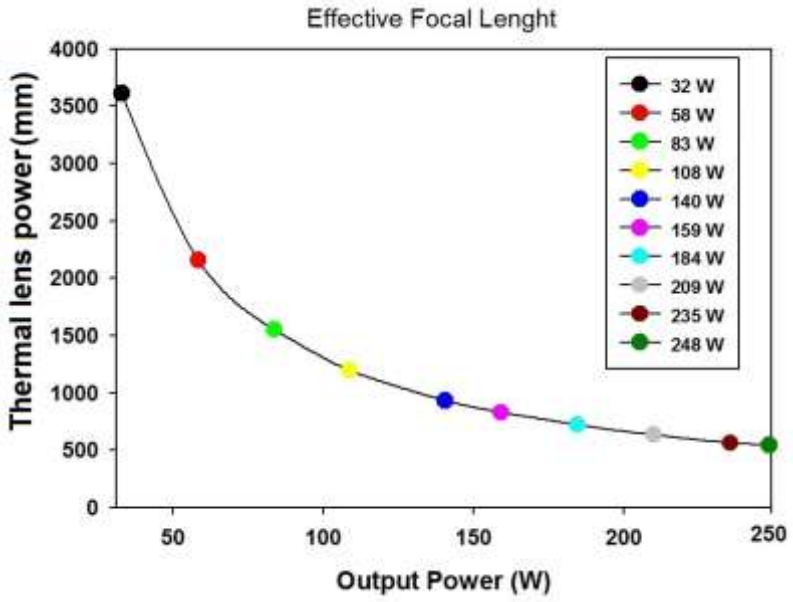


Figure 15. The effective focal length of the thermal lens corresponding to different output powers.

## VIII. OUTPUT AND BEAM QUALITY RESULTS

In the last section, we have used Dynamic Multimode Analysis (DMA) method to calculate our output power respect to multimode operation. To end to this, the optimization of laser cavity with the goals of high beam quality has been done simultaneously. To obtain this result we simulated different configurations by changing the length of the cavity for the pump power of 1000W. Then, a linear plano-concave cavity with an output coupler of 1m with refection of 88% has been taken into account. The simulation result is shown in Fig.16. After that, by using the optimized length of the cavity from previous section, we continued the simulation for different pump powers. The average optical to optical efficiency of 35% for our modeling is obtained as shown in Fig.17.

Furthermore, the slope efficiency of our modeling which is defined as the ratio of the absorbed pump power inside the crystal domain to the out power is obtained 52.5% Fig.18.

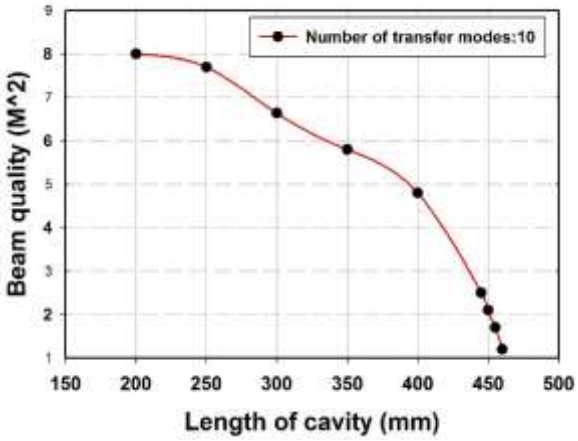


Figure 16. Optimizing the length of the cavity respect to thehigh beam quality

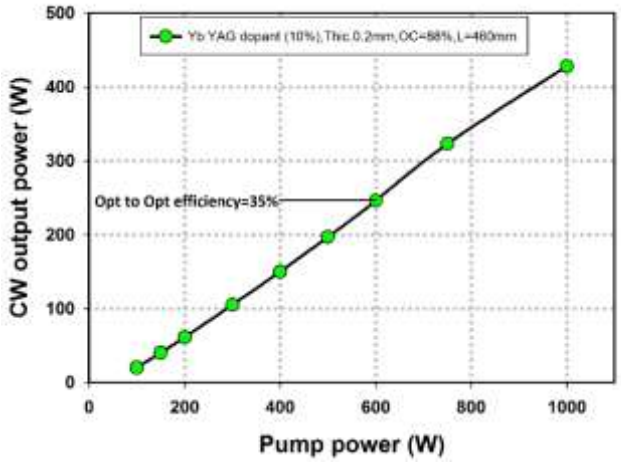


Figure 17. Pump power versus output power (optical to optical effciency) for Yb:YAG dopant of 10%

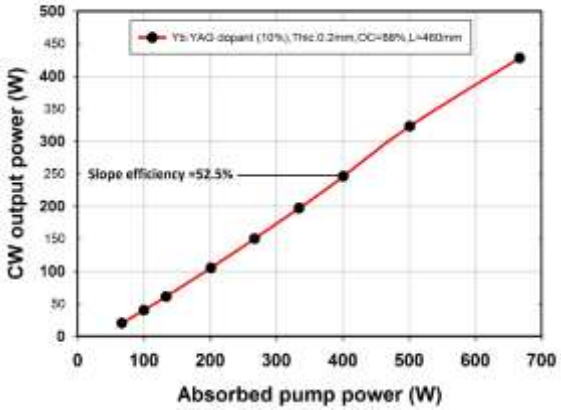


Figure 18. Absorbed pump power versus output power (slope efficiency) for Yb:YAG dopant of 10%

Finally, to optimizing the output coupler reflectivity of our system respect to the high beam quality has been done correspondingly. We used the previous optimization results either to improve the output power or to keep the high beam quality of our delivery system. The result of this investigation is shown in Fig.19. As shown in Fig.19, the optimum result of the output coupler reflectivity obtained for 88% for the beam quality of 1.1 in

multimode operation. The output TEM00 profile on the back mirror (bottom surface of the disk) is depicted in Fig.20.

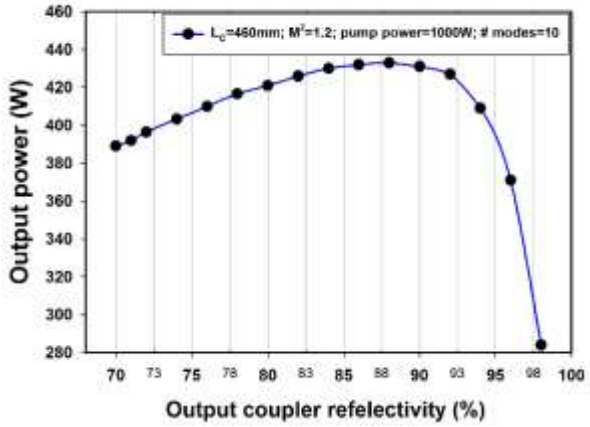


Figure 19. Optimizing the output coupler reectivity respect to the output power

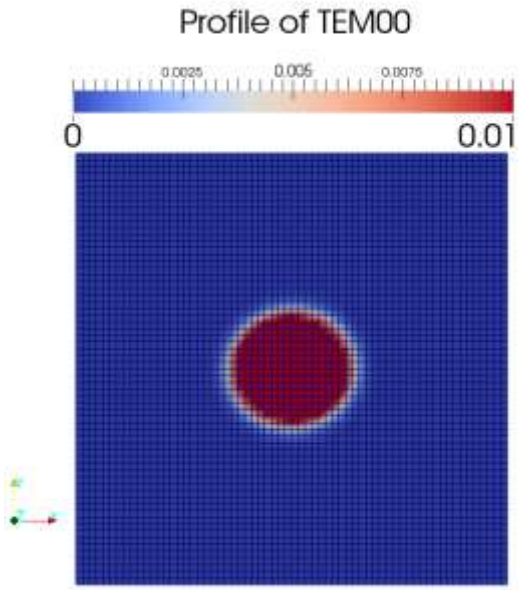


Figure 20. TEM00 profile on the front mirror

## IX. CONCLUSION

In this paper, we have used ray tracing method and finite element analysis (FEA) to simulate and calculate the distributions of absorbed pump power density and opto-mechanical properties such temperature, Von Mises stress and deformation distribution in three dimensional of edged-pumped trapezoid Yb:YAG/YAG thin disk laser. Due to the specific shape of our active medium, we optimized the efficient thickness and Yb:YAG dopant using FEA in our laser simulation code software ASLD. Furthermore, according to our modeling, we have shown that the center of our disk are sensitive part concerning induced thermal effects in high pump power. As expressed inside the script the most significant parameters that cause thermal lensing effect, are temperature-dependent refractive index and the deformation of the disk which are both directly related to the temperature distribution inside the crystal. Our modeling shows that the OPD inside the crystal varies from -3613.74mm to -542.85mm in the output power range of 30W to 250W. Based on the results of this work it could be possible to design the proper resonators compensating thermal lensing effect inside the cavity and increase the out beam quality factor. So, we simulated different configurations of linear cavity with different lengths and different output curvatures to optimize both the output power and beam quality of our laser system. To end this, we used Dynamic Multimode Analysis (DMA) method to calculate the output power respect to different pump powers, different output coupler reflectivity and other parameters in multimode operation. Finally, we optimized our modeling for the pump power of 1000W with the beam the quality of 1.1.

## ACKNOWLEDGMENT

The authors gratefully acknowledge funding of the Erlangen Graduate School in Advanced Optical Technologies (SAOT) by the German Research Foundation (DFG) in the framework of the excellence initiative.

## REFERENCES

[1] A.Giesen, H. Hügel, A. Voss, K. Wittig, U. Brauch, H.Opower, "Scalable concept for diode-pumped high-power solid state lasers", Applied Physics B, 58 1994.

[2] S. Erhard, A.Giesen, M.Karszewski, T.Rupp, C.Stewen, I.Johannsen, and K.Contag,"Novel Pump Design of Yb:YAG Thin Disc Laser for Operation at Room Temperature with Improved Efficiency",Conference Paper Advanced Solid State Lasers Boston, Massachusetts 1999.

[3] K.Contag, M.Larionov, A.Giesen, H.Hugel , "A 1-kW CW thin disc laser", Selected Topics in Quantum Electronics, IEEE 2000.

[4] B. Weichelt, D. Blazquez-Sanchez, A. Austerschulte, A.Voss, T. Graf, A. Killi, "Improving the brightness of a multi-kilowatt single thin-disk laser by an aspherical phase front correction", Optics Letters, Vol. 36, Issue 6, 2011 pp.799801.

[5] M.E. Innocenzi, H.T. Yura, C.L. Fincher and R.A. Fields, "Thermal modeling of continuouswave endpumped solidstate lasers", Applied Physics Letters, Vol. 56, Issue 19 1990 pp.799801.

[6] S. Chenais, F. Druon , S. Forget , F. Balembois, P.Georges, "On thermal effects in solid state lasers: the case of ytterbium-doped materials", Progress in quantum electronics 30 2006.

[7] F. Song, C. Zhang, X. Ding, J. Xu, G. Zhang, M. Leigh and N. Peyghambarian, "Determination of thermal focal length and pumping radius in gain medium in laser diode pumped Nd:$YVO_4$ lasers" , Appl. Phys. Lett.81, 2002.

[8] N. U. Wetter, E. P. Maldonado and N. D. Vieira, "Output Power Characteristics of Solid State Lasers with Thermal Lensing and High $TEM_{00}$ Mode Volume" , Revista de Fsica Aplicada e Instrumentaco, Vol.13, No.2, 1998 P.3437.

[9] J.Mende, J. Speiser, G. Spindler, W. L. Bohn, A. Giesen, "Mode dynamics and thermal lens effects of thin-disk lasers", Proc. SPIE 6871, Solid State Lasers XVII: Technology and Devices, 68710M 2008.

[10] M. Tsunekane and T. Taira, "High-Power Operation of Diode Edge-Pumped, Glue-Bonded, Composite Yb:$Y_3Al_5O_{12}$ Microchip Laser with Ceramic, Undoped YAG Pump Light-Guide", Jpn. J. Appl. Phys. 44 L1164 2005.

[11] R. Fu, G. Wang, Z. Wang, E. Ba, G. Mu and X.Hua Hu, "Design of efficient lens ducts", Applied Optics, Vol. 37, Issue 18, 1998.

[12] RJ. Beach,"Theory and optimization of lens ducts", Appl Opt. Apr 20 ,35(12) 1996 P.200515.

[13] T. Dascalu, T. Taira, "Highly efficient pumping configuration for microchip solid-state laser", Opt Express.23 14(2) 2006 P.6707.

[14] M. Tsunekane, T. Dascalu and T. Taira , "High Power Operation of Diode Edge-Pumped, Composite Microchip Yb:YAG Laser with Ceramic Pump Wave Guide" , Conference Paper Advanced Solid-State Photonics , Vienna,Austria.23 14(2) 2005 P.6707.

[15] H.Aminpour, I.M. Asl, J.Sabbaghzadeh and S.Kazemi , "Simulation and design of applied hollow-duct used for side-pumped cutting-edged of high power disk laser",Optics Communications 283(23) 2010 P:4727-4732.

[16] S. Toroghi, A.K. Jafari and A.H. Golpayegani, "A model of lasing action in a quasi-four level thin active media", IEEE J. Quantum Electron 46,(6) 2010 P.871876.

[17] J. Foster and L. M.Osterink, "Index of refraction and expansion thermal coefficients of Nd:YAG", Opt Express. 7, 1998 P.2428 - 2439.

[18] www.asldweb.com ASLD GmbH,Erlangen,Germany.

[19] www.lambdares.com

[20] A.Bejan, "Heat Transfer",Wiley 1993 P.704

[21] Y.S. Huang, H.L. Tsai, F.L. Chang, "Thermo-optic effects affecting the high pump power end pumped solid state lasers: Modeling and analysis" ,Optics Communications 273 2007 P.515525.

[22] B. Bendow, P. Gianino, "Optics of thermal lensing in solids", Appl Opt. 1;12(4) 1973.

[23] E.Wyss, M. Roth, T.Graf, H.P.Weber,"Thermo optical compensation methods for high-power lasers", Quantum Electronics, IEEE Journal of Vol.38 2002 P.1620 -1628.

[24] A. Soloviev, I. Snetkov, V. Zelenogorsky, I. Kozhevatov, O. Palashov and E. Khazanov, "Experimental study of thermal lens features in laser ceramics", Optics Express, Vol. 16, Issue 25, 2008 pp.21012-21021.

[25] J. Frauchiger, P.Albers, H.P.Weber, "Modeling of thermal lensing and higher order ring mode oscillation in end-pumped CW Nd:YAG lasers", Quantum Electronics, IEEE Vol.:28 , Issue:4 1992 P.1046-1056.

[26] Y.F. Chen, C.F.Kao, T.M.Huang, C.L.Wang, S.C.Wang, "Influence of thermal effect on output power optimization in fiber coupled laser-diode end- pumped lasers", Quantum Electronics, IEEE Volume:3 , Issue: 1 1997.